and no-phonon levels, and one would generally expect an enhancement of the polaron self-energy. A more detailed study of these neighborhoods may yet reveal such effects.

In this work, we have ignored the possibility of an anisotropy in the conduction-band levels except to take the precaution to always orient the samples with **H** along ⟨110⟩. The main effect is expected to be in the g factor. The theoretical results[43] and the experimental results of McCombe[44] indicate that the anisotropy of the conduction-band g factor for the two lowest Landau levels is less than 4% for $H<40$ kG. For the lowest Landau level, the anisotropy is less than 2%. The anisotropy alone cannot account for a 10% remote-band contribution to the g factor.

An interesting subject for further work is to attempt to reconcile the results of this work (*intraband* transitions) with the work on the *interband* magnetoabsorption spectrum of InSb. Pidgeon-Brown type of analysis of *interband* absorption gives a conduction-band mass that lies outside of the experimental uncertainty of the *intraband* value. A detailed reexamination of the analysis of each of the experiments is needed. However, the discrepancy appears to be real and seems to indicate that there is something fundamentally different between the energy levels involved in the *intraband* experiments and those involved in the *interband* experiments in addition to effects due to excitons. A similar discrepancy appears to exist in the case of gray tin.[45]

[43] N. R. Ogg, Proc. Phys. Soc. (London) **89**, 431 (1966).
[44] B. D. McCombe, Solid State Commun. **6**, 553 (1968).

ACKNOWLEDGMENTS

It is with appreciation that we acknowledge the excellent assistance of M. J. Fulton and P. L. Ligor in carrying out the experimental work. Without their exceptional effort in preparing the samples and their meticulousness in achieving maximum performance from each part of the spectrometer system, most of the data could not have been obtained. We also acknowledge crucial discussions concerning the interpretation with L. M. Roth, H. J. Zeiger and D. M. Larsen.

[45] S. H. Groves (private communication).

PHYSICAL REVIEW B VOLUME 1, NUMBER 6 15 MARCH 1970

Calculation of the Optical Constants of PbTe from Augmented-Plane-Wave k·p Energy Bands*

DENNIS D. BUSS† AND NELSON J. PARADA‡
Department of Electrical Engineering and Center for Materials Science and Engineering, Massachusetts Institute of Technology, Cambridge, Massachusetts 02139
(Received 29 May 1969; revised manuscript received 1 August 1969)

The augmented-plane-wave method has been used to calculate the energies and wave functions of eleven levels at the origin of the Brillouin zone (BZ) of PbTe. From the wave functions, momentum matrix elements have been calculated and these have been used in a **k·p** expansion of the energy bands. The **k·p** secular equation has been solved throughout the BZ and the results have been used to calculate the interband contribution to the optical constants in the random-phase approximation. The calculated value of $\epsilon_1(\omega=0)$ (40.0) compares favorably to the measured value ($\epsilon_\infty=31.8$), and the calculated reflectivity agrees with experiment to within 10% in the frequency range $0<\hbar\omega<3$ eV.

I. INTRODUCTION

In order to make a calculation of the optical dielectric constant $\epsilon(\omega)=\epsilon_1(\omega)+i\epsilon_2(\omega)$ of a material, it is necessary to know the resonant frequency and the oscillator strength of every transition in the material, that is, it is necessary to know the energy differences between the occupied and the unoccupied bands everywhere in **k** space, and the momentum matrix elements coupling these bands. Therefore, by comparing these calculations with measured optical properties, it is possible to test the validity of the wave functions from which momentum matrix elements are calculated as well as the accuracy of the energy bands.

First-principles calculations are capable of yielding the information required to calculate optical constants. For example, Herman *et al.* have used a combination of the orthogonalized-plane-wave (OPW) method and the pseudopotential method to obtain the optical spectrum of many materials including the Pb salts.[1] OPW energy bands are calculated at a few high-symmetry points and pseudopotential band parameters are adjusted to fit the OPW results. Optical properties are then obtained from the pseudopotential bands either by as-

* Work supported in part by the National Science Foundation and in part by the U. S. Army Research Office (Durham).
† Present address: Central Research Laboratory, Texas Instruments Inc., Dallas, Tex.
‡ Present address: Departamento de Fisica, Universidade de Sao Paulo, Sao Paulo, Brazil.

[1] F. Herman, R. L. Kortum, I. B. Ortenburger, and J. P. Van Dyke, J. Phys. (Paris), Suppl. **29**, 62 (1968), and references cited here.

suming the momentum matrix elements to be constant everywhere in the Brillouin zone (BZ) or by calculating them for pseudo-wave functions.

Of course, better energy bands can be obtained by adjusting parameters in a band model to fit empirically determined features of the energy bands. The empirical-pseudopotential method has been widely used[2] and has recently been applied to the calculation of the optical constants of PbTe and related compounds.[3] Two other empirical schemes which have been successful in explaining the spectrum of some materials are the tight-binding method[4] and the $\mathbf{k}\cdot\mathbf{p}$ method.[5] As Herman *et al.*[6] have pointed out, however, empirical schemes depend upon a correct interpretation of the experimental spectrum, and a first-principles calculation is useful in assigning features of the optical spectrum to features of the energy-band structure.

A first-principles calculation of the absorption coefficient of PbTe has recently been reported.[7] In this calculation, a parabolic-band approximation has been made for the bands in the vicinity of the L point, and the absorption in the vicinity of the edge has been calculated. Agreement with experiment[8,9] is best near the fundamental edge. For higher frequencies, however, the calculated absorption is an order of magnitude too small, indicating the importance of transitions at points other than L.

In the present work, an improvement of the augmented-plane-wave (APW) calculation of Conklin *et al.*[10] was used to obtain energies and wave functions for eleven levels in PbTe at $\mathbf{k}=0$. Momentum matrix elements were calculated from the APW wave functions and the energies and momentum matrix elements were used in a $\mathbf{k}\cdot\mathbf{p}$ secular equation to obtain the energies and wave functions everywhere in the BZ.[11] From these, the interband contribution to the electronic dielectric constant was obtained for frequencies below 5 eV.

TABLE I. Energy in rydbergs for the eleven levels at Γ used in the $\mathbf{k}\cdot\mathbf{p}$ calculation. Where more than one band transforms according to a particular representation, the bands are arbitrarily labeled with a preceding superscript. The parenthesis gives the single-group representation which characterizes the level in the absence of spin-orbit interaction.

$^2\Gamma_8^+(\Gamma_{12})$	−0.04098
$^2\Gamma_6^+(^2\Gamma_1)$	−0.03933
$\Gamma_7^-(\Gamma_2')$	−0.08594
$\Gamma_7^+(\Gamma_{25}')$	−0.14450
$^1\Gamma_8^+(\Gamma_{25}')$	−0.14450
$^2\Gamma_8^-(^2\Gamma_{15})$	−0.26215
$^2\Gamma_6^-(^2\Gamma_{15})$	−0.39062
Gap	
$^1\Gamma_8^-(^1\Gamma_{15})$	−0.65966
$^1\Gamma_6^-(^1\Gamma_{15})$	−0.73552
$^1\Gamma_6^+(^1\Gamma_1)$	−1.00995
$^3\Gamma_6^+(^3\Gamma_1)$	−1.47777

Calculation of the optical constants of PbTe is complicated by the fact that transitions responsible for the optical properties occur at quite low energies, and hence, small errors in the band energies are large percentage errors and result in large errors in the optical constants. Moreover, interpretation of the experimental spectrum is complicated by the fact that contributions to the peaks in the joint density of states come from a large region of $\mathbf{k}$ space,[1] and these peaks are only indirectly related to the many critical points in the joint density of states.

This calculation was undertaken to test the validity of the APW results and to provide a framework for the interpretation of the optical spectrum. The $\mathbf{k}\cdot\mathbf{p}$ energy bands are presented in Sec. II and the calculation of the optical constants is presented in Sec. III. In Sec. IV, the experimentally measured optical properties are discussed in the light of the calculation.

II. k·p ENERGY BANDS IN PbTe

If the energies of all bands at some particular $\mathbf{k}_0$ are known, and if matrix elements coupling these bands are known at $\mathbf{k}_0$, then the energy bands and momentum matrix elements can be computed everywhere in the zone by solving the $\infty\times\infty$ secular equation[11]

$$\det[H^{\mathbf{k}\cdot\mathbf{p}}(\mathbf{k})-\lambda]=0, \tag{1}$$

where

$$H_{ij}^{\mathbf{k}\cdot\mathbf{p}}(\mathbf{k})=\left[E_i(\mathbf{k}_0)+\frac{\hbar^2\kappa^2}{2m}\right]\delta_{ij}+\frac{\hbar}{m}\boldsymbol{\kappa}\cdot\mathbf{p}_{ij}. \tag{2}$$

The $E_i(\mathbf{k}_0)$ are the energies at $\mathbf{k}_0$, $\mathbf{p}_{ij}$ are matrix elements of momentum coupling the bands i and j at $\mathbf{k}_0$, and $\boldsymbol{\kappa}=\mathbf{k}-\mathbf{k}_0$.

The relativistic APW method[10] has been used to obtain the energies and wave functions at $\mathbf{k}_0=(0,0,0)$ of 30 states counting the Kramers degeneracy (eleven levels at Γ), and the wave functions were used to calculate all momentum matrix elements coupling these

[2] M. L. Cohen and T. K. Bergstresser, Phys. Rev. **141**, 789 (1966); W. Saslow, T. K. Bergstresser, C. Y. Fong, and M. L. Cohen, Solid State Commun. **5**, 667 (1967), and references cited here.

[3] P. J. Lin, W. Saslow and M. L. Cohen, Solid State Commun. **5**, 893 (1967) (SnTe); Y. W. Tung and M. L. Cohen, Phys. Rev. **180**, 823 (1969) (SnTe, GeTe, PbTe); Y. Tsang and M. L. Cohen (unpublished) (PbTe).

[4] G. Dresselhaus and M. S. Dresselhaus, Phys. Rev. **160**, 649 (1967); G. Dresselhaus, Solid State Commun. **7**, 419 (1969).

[5] C. W. Higginbotham, F. H. Pollak, and M. Cardona, Solid State Commun. **5**, 513 (1967).

[6] F. Herman, R. L. Kortum, C. D. Kuglin, and J. L. Shay, *II–VI Semiconducting Compounds, 1967 International Conference* (W. A. Benjamin, Inc., New York, 1967), p. 503.

[7] P. T. Bailey, M. W. O'Brien, and S. Rabii, Phys. Rev. **179**, 735 (1969).

[8] W. W. Scanlon, in *Solid State Physics*, edited by F. Seitz and D. Turnbull (Academic Press Inc., New York, 1959), Vol. 9, p. 83; J. Phys. Chem. Solids **8**, 423 (1959).

[9] M. Cardona and D. L. Greenaway, Phys. Rev. **133**, A1685 (1964).

[10] J. B. Conklin, Jr., L. E. Johnson, and G. W. Pratt, Jr., Phys. Rev. **137**, A1282 (1965).

[11] For a review of the $\mathbf{k}\cdot\mathbf{p}$ method see E. O. Kane, in *Semiconductors and Semimetals*, edited by R. K. Willardson and A. C. Beer (Academic Press Inc., New York, 1966), Vol. 1, Chap. 3.

TABLE II. Matrix elements of p_x, p_y and p_z between double-group representations at Γ. The second subscript on Γ labels the partners. Matrix elements not tabluated explicitly can be obtained from those given here by applying time reversal. ($a=1/\sqrt{3}$; $b=1/\sqrt{2}$; $c=1/\sqrt{6}$; $d=\frac{1}{3}$.)

	$\Gamma_{6,1}^-(\Gamma_{15})$	$\Gamma_{6,2}^-(\Gamma_{15})$	$\Gamma_{7,1}^-(\Gamma_2')$	$\Gamma_{7,2}^-(\Gamma_2')$	$\Gamma_{8,1}^-(\Gamma_{15})$	$\Gamma_{8,2}^-(\Gamma_{15})$	$\Gamma_{8,3}^-(\Gamma_{15})$	$\Gamma_{8,4}^-(\Gamma_{15})$
	0	$-iaM_{1,15}$	0	0	$-ibM_{1,15}$	0	$icM_{1,15}$	0
$\Gamma_{6,1}^+(\Gamma_1)$	0	$-aM_{1,15}$	0	0	$bM_{1,15}$	0	$cM_{1,15}$	0
	$-iaM_{1,15}$	0	0	0	0	$2icM_{1,15}$	0	0
	0	0	0	$iaM_{25,2}$	$icM_{25,15}$	0	$ibM_{25,15}$	0
$\Gamma_{7,1}^+(\Gamma_{25}')$	0	0	0	$aM_{25,2}$	$cM_{25,15}$	0	$-bM_{25,15}$	0
	0	0	$iaM_{25,2}$	0	0	0	0	$2icM_{25,15}$
	$-ibM_{25,15}$	0	$-icM_{25,2}$	0	0	0	0	$-iaM_{25,15}$
$\Gamma_{8,1}^+(\Gamma_{25}')$	$-bM_{25,15}$	0	$cM_{25,2}$	0	0	0	0	$aM_{25,15}$
	0	0	0	$-2icM_{25,2}$	$-iaM_{25,15}$	0	0	0
	$icM_{25,15}$	0	$-ibM_{25,2}$	0	0	$-iaM_{25,15}$	0	0
$\Gamma_{8,3}^+(\Gamma_{25}')$	$-cM_{25,15}$	0	$-bM_{25,2}$	0	0	$aM_{25,15}$	0	0
	0	$2icM_{25,15}$	0	0	0	0	$-iaM_{25,15}$	0
	$iaM_{12,15}$	0	0	0	0	$icM_{12,15}$	0	$-ibM_{12,15}$
$\Gamma_{8,1}^+(\Gamma_{12})$	$aM_{12,15}$	0	0	0	0	$cM_{12,15}$	0	$bM_{12,15}$
	0	0	0	0	0	0	0	0
	$-idM_{12,15}$	0	0	0	0	$-idbM_{12,15}$	0	$icM_{12,15}$
$\Gamma_{8,3}^+(\Gamma_{12})$	$dM_{12,15}$	0	0	0	0	$dbM_{12,15}$	0	$cM_{12,15}$
	0	$-2idM_{12,15}$	0	0	0	0	$-4idbM_{12,15}$	0

states. The exact $\infty\times\infty$ secular equation was then approximated by a 30×30 secular equation which factors immediately into two 15×15 secular equations by the symmetry of time reversal and inversion.

The band parameters used in the calculation are given in Tables I–III. Table I gives the eleven energy levels at Γ. Table II shows how matrix elements of p_x, p_y, and p_z between double-group states are related to matrix elements $M_{i;j}$ between corresponding single-group states. Table III gives the values of $M_{i;j}^{n;m}$ obtained in this work. The particulars of this calculation are presented elsewhere,[12] and the results are displayed in Fig. 1 along with the APW results of Ref. 10.

Since the $\mathbf{k}\cdot\mathbf{p}$ method expresses eigenfunctions at $\mathbf{k}$ as linear combinations of (eigenfunctions at Γ)$\times(e^{i\mathbf{k}\cdot\mathbf{r}})$, matrix elements of momentum between eigenfunctions at $\mathbf{k}$ can be written as linear combinations of matrix elements between states at Γ. If the transformation $U(\mathbf{k})^\dagger H^{\mathbf{k}\cdot\mathbf{p}}U(\mathbf{k})$ diagonalizes $H^{\mathbf{k}\cdot\mathbf{p}}$, then

$$\mathbf{p}_{ij}(\mathbf{k})=\sum_{nm}U_{ni}^*(\mathbf{k})\mathbf{p}_{nm}(\mathbf{k}_0)U_{mj}(\mathbf{k}),\quad i\neq j. \tag{3}$$

No approximation is necessary beyond the truncation of the secular equation.

TABLE III. Values for $M_{i;j}^{n;m}$ which were used in the $\mathbf{k}\cdot\mathbf{p}$ calculation.

$M_{1;15}^{n;m}=\langle{}^n\Gamma_1|p_x|{}^m\Gamma_{15,1}\rangle$: $M_{12;15}^{1;m}=\langle\Gamma_{12,1}|p_x|{}^m\Gamma_{15,1}\rangle$:
$M_{25;2}=\langle\Gamma_{25,1}'|p_x|\Gamma_2'\rangle$: $M_{25,15}^{1;m}=\langle\Gamma_{25,2}'|p_x|{}^m\Gamma_{15,3}\rangle$.

Matrix elements (a.u.)	
$M_{1;15}^{1;1}$	0.4845
$M_{1;15}^{1;2}$	0.1250
$M_{1;15}^{2;1}$	−0.0775
$M_{1;15}^{2;2}$	0.5900
$M_{1;15}^{3;1}$	0.2185
$M_{1;15}^{3;2}$	−0.1125
$M_{12;15}^{1;1}$	0.2185
$M_{12;15}^{1;2}$	0.5945
$M_{25;2}$	0.4745
$M_{25;15}^{1;1}$	0.6165
$M_{25;15}^{1;2}$	0.2660

The magnitude squared of momentum matrix elements coupling the uppermost valence band with the lowermost conduction band is shown in Fig. 2. Two important observations can be made from this figure: (1) The approximation $|\langle\text{cond}|\mathbf{p}|\text{val}\rangle|^2$ which is constant throughout the BZ is clearly not valid for PbTe. At points in $\mathbf{k}$ space where the conduction and valence bands almost cross, the momentum matrix element is very large giving rise to what Phillips, in a slightly different context, calls umklapp-enhanced oscillator strength.[13] (2) The momentum matrix elements coupling valence and conduction bands at and near L are small, partly accounting for the fact that the transitions in the vicinity of L do not contribute strongly to the optical properties above the gap frequency.

III. CALCULATION OF OPTICAL CONSTANTS

$\epsilon(\omega)$ is calculated in the random-phase approximation using the following expression[14]:

$$\epsilon(\omega,0)=1-\frac{4\pi e^2}{\Omega}\times\sum_{\mathbf{k}}\sum_{ij}\frac{|\langle i\mathbf{k}|p^\nu|j\mathbf{k}\rangle|^2[f_0(E_{\mathbf{k},j})-f_0(E_{\mathbf{k},i})]}{m^2\omega_{ij}^2[E_{\mathbf{k},j}-E_{\mathbf{k},i}-\hbar\omega-i\hbar/\tau_{ij}]}, \tag{4}$$

[12] G. W. Pratt, Jr., and N. J. Parada, Int. J. Quantum Chem. **Is**, 589 (1967); N. J. Parada, Ph.D. thesis, MIT, 1968 (unpublished).

[13] J. C. Phillips, in *Solid State Physics*, edited by F. Seitz and D. Turnbull (Academic Press Inc., New York, 1966), Vol. 18, p. 70.

[14] H. Ehrenreich and M. H. Cohen, Phys. Rev. **115**, 786 (1959).

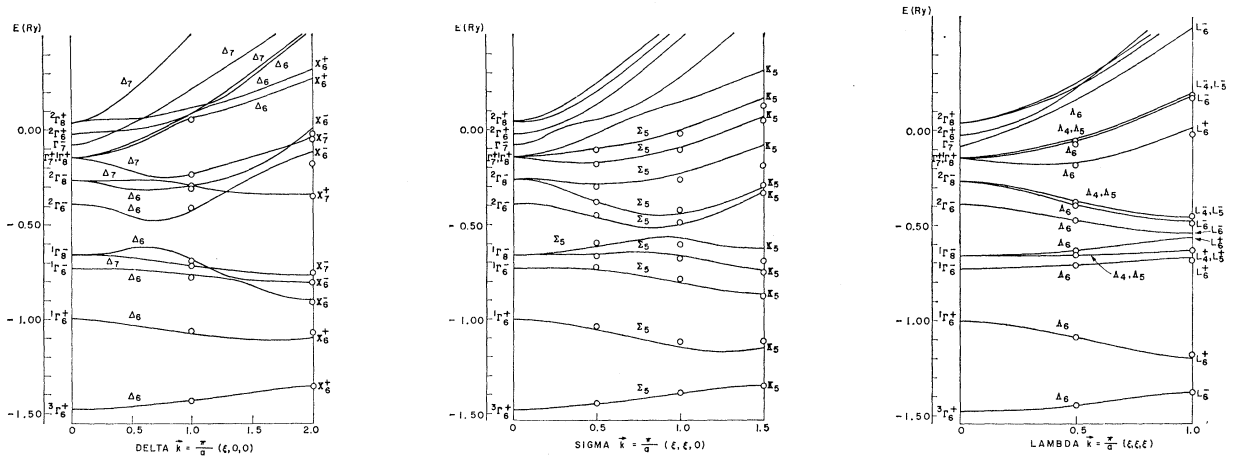

(a) (b) (c)

FIG. 1. The $\mathbf{k}\cdot\mathbf{p}$ energy bands along the three principle directions in $\mathbf{k}$ space. The circles give the results of the APW calculation for comparison.

where Ω is the unit-cell volume, $\hbar\omega_{ij}=E_{\mathbf{k},i}-E_{\mathbf{k},j}$, and p^ν is the operator for linear momentum in the ν direction. For a cubic material, the dielectric response is isotropic (i.e., independent of direction i_ν), and in order to make the expression under the summation invariant under the operations of the point group of the crystal (O_h), $|\langle i\mathbf{k}|p^\nu|j\mathbf{k}\rangle|^2$ was replaced by $\frac{1}{3}|\langle i\mathbf{k}|\mathbf{p}|j\mathbf{k}\rangle|^2 \equiv\frac{1}{3}\sum_\nu|\langle i\mathbf{k}|p^\nu|j\mathbf{k}\rangle|^2$. We have neglected the intraband term in the expression given in Ref. 14 because we are dealing with intrinsic PbTe in which no carriers are excited. The f's in Eq. (4) are Fermi functions which have been evaluated at $T=0°$K in this calculation.

The imaginary part h/τ_{ij} of the energy difference is actually a function of $\mathbf{k}$ and of band indices. In this calculation, however, it has been treated as a constant equal to 0.005 Ry which corresponds to $\tau_{ij}(\mathbf{k})=\tau =6\times10^{-14}$ sec. τ was chosen to be sufficiently small that it had negligible effect upon the result other than to smooth out the integration. This value of τ is not inconsistent with the order of magnitude estimate which can be made from scattering lifetimes of electrons and holes.

The summation on bands in Eq. (4) has been restricted for this calculation to the three twofold degenerate bands on either side of the gap. This restriction excludes certain bands which lie within 5 eV of the gap and thus limits the validity of the calculation to the frequency range 0–5 eV. The error introduced by ignoring these bands is expected to be small at low frequencies. As can be seen from Eq. (4), however, the error should increase with increasing frequency and become large for $\hbar\omega\simeq5$ eV. There are, in this approximation, nine transitions for which energy differences and momentum matrix elements have been calculated throughout the BZ.[15]

[15] Each one of these nine transitions is actually four transitions, because each of the three valence bands and each of the three conduction bands is twofold degenerate. The momentum matrix elements squared for the four transitions have been added to give an effective matrix element, and it is this quantity which is plotted in Fig. 2.

The summation on $\mathbf{k}$ over the entire BZ was reduced by symmetry to a summation over 1/48 of the zone,[16] which is possible because the summand is invariant under the operations of the group O_h. In this reduced region, the energy differences and momentum-matrix-elements squared were calculated at 152 evenly spaced points, and the values between these points were obtained by linear interpolation. The error which was introduced by making the linear interpolation was estimated to be approximately 20%, an estimate made by determining the *LCAO* bands in PbTe, and by using the method of Ref. 4 to obtain the optical properties. Since nonrelativistic bands were used in this estimate, it was feasible to carry out the integration on $\mathbf{k}$ space by evaluating the integrand at every point directly, thereby avoiding the linear interpolation. The same calculation was performed using the linear interpolation and the results were compared.

The summation over 1/48 of the BZ was carried out by dividing this region into small boxes, some of which were found to contribute strongly to the sum, while others were found to contribute very little. Within each box a Monte Carlo integration was performed, that is,

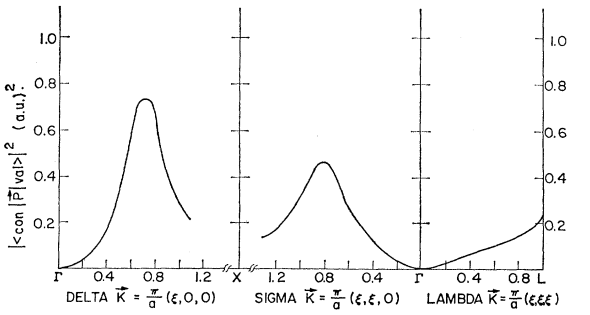

FIG. 2. The magnitude squared of the momentum matrix element between the highest valence band and the lowest conduction band, along the three principle directions in $\mathbf{k}$ space. See Ref. 15. Momentum is expressed in atomic units.

[16] D. Brust, Phys. Rev. **134**, A1337 (1964).

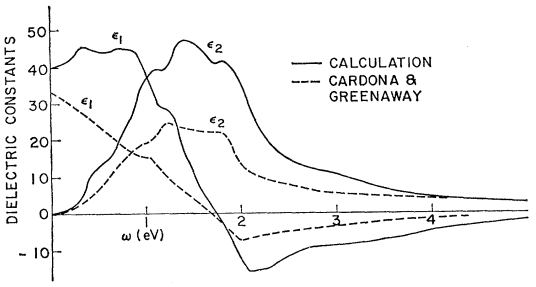

FIG. 3. The calculated complex dielectric constant $\epsilon(\omega)=\epsilon_1(\omega)+i\epsilon_2(\omega)$ compared with the results obtained by performing a Kramers-Kronig analysis on the measured reflectivity.

points were generated at random within each box, at each point the integrand was evaluated, these values were added together, and the total was divided by the number of random points. The integration was continued until convergence was obtained, i.e., until the answer after N_p random points differed from the answer after $\frac{1}{2}N_p$ random points by 0.1 or less. Using this convergence criterion, boxes which contribute strongly required a large number of points ($\sim$2000), and boxes which contribute only slightly required very few points (50 or less). A total of 11 850 random points and approximately $1\frac{1}{2}$ h of IBM 360 65/40 time were required to perform all integrations. The final answer for $\epsilon(\omega)$ was obtained by simply adding together the contributions from the different boxes.

The calculated values of $\epsilon(\omega)=\epsilon_1(\omega)+i\epsilon_2(\omega)$ are shown in Fig. 3 along with the results of Ref. 9. In Fig. 4, calculated real and imaginary parts of the complex index of refraction $N(\omega)=n(\omega)+ik(\omega)$ ($N^2=\epsilon$) are compared with experiment.[9,17] The calculation agrees to within 20% with the experimental results at $\omega=0$, but deviates significantly for $\omega>0$.

IV. COMPARISON WITH EXPERIMENT

The experimental values of ϵ and N which are shown in Figs. 3 and 4 are obtained by measuring the intensity of light reflected from a PbTe crystal.[9,17] The reflectivity R is the ratio of reflected intensity to incident intensity and contains no information about the phase change θ that the radiation experiences on reflection

$$R=\left|\frac{\mathbf{E}_{\rm ref}}{\mathbf{E}_{\rm inc}}\right|^2=\left|\frac{1-N}{1+N}\right|^2=\frac{(n-1)^2+k^2}{(n+1)^2+k^2}. \quad (5)$$

Of course n and k are related by the Kramers-Kronig (KK) relations. If R is known for all frequencies, then θ can be calculated from the Bode integral,[18] and n and k or ϵ_1 and ϵ_2 can be determined uniquely. The reflectivity has been measured, however, only for $\hbar\omega<25$ eV, and an extrapolation has been made for higher frequencies.[9] This introduces the possibility of error into the analysis.[19] Direct measurement of the phase angle θ for reflection from Ge has verified the validity of the KK analysis for this material,[20] but similar measurements have not been made for PbTe.

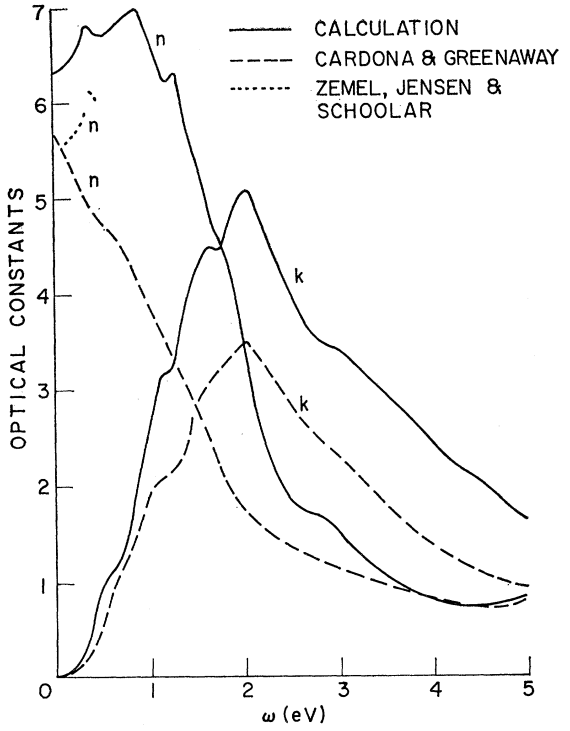

FIG. 4. The calculated index of refraction $N(\omega)=n(\omega)+ik(\omega)$ compared with the results obtained by performing a Kramers-Kronig analysis on the measured reflectivity.

A striking feature of both Figs. 3 and 4 is that, at $\omega=0$, the calculated values of n and ϵ_1 agree quite well with the experimental values given in Ref. 9. This would be true even if the KK analysis were in error because at $\omega=0$, $\epsilon_2=k=0$, and both ϵ_1 and n are determined unambiguously from the experimentally measured reflectivity at $\omega=0$. A comparison with direct measurements has been made by using the calculated values of n and k to obtain the reflectivity. This comparison, shown in Fig. 5, indicates excellent agreement out to about 3 eV, but the agreement slowly deteriorates at higher frequencies and for $\hbar\omega>5$ eV, the approximations made in Sec. III invalidate the result.

The absorption coefficient $\alpha(\omega)=2k(\omega)\omega/c$, obtained using the optical constants of Figs. 3 and 4, is shown in Fig. 6, along with the results of others.[7–9] Only the shape of the dashed curve of Fig. 6 is experimentally

[17] J. N. Zemel, J. D. Jensen, and R. B. Schoolar, Phys. Rev. **140**, A330 (1965).

[18] H. R. Philipp and E. A. Taft, Phys. Rev. **113**, 1002 (1959).

[19] Because of the extrapolation above 25 eV, the authors of Ref. 9 regard the results of the KK analysis as approximate. R. B. Schoolar and J. R. Dixon, Phys. Rev. **137**, A667 (1965), footnote 11.

[20] R. F. Potter, in *Proceedings of the International Conference on the Physics of Semiconductros, Kyoto* (The Physical Society of Japan, Tokyo, 1966), p. 107.

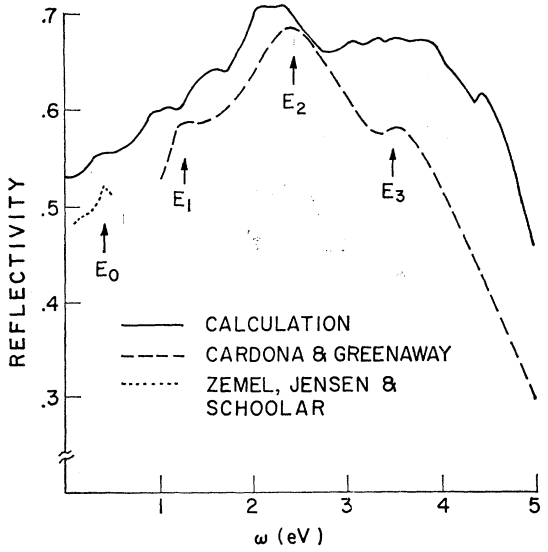

FIG. 5. The calculated and measured reflectivity $R(\omega)$.

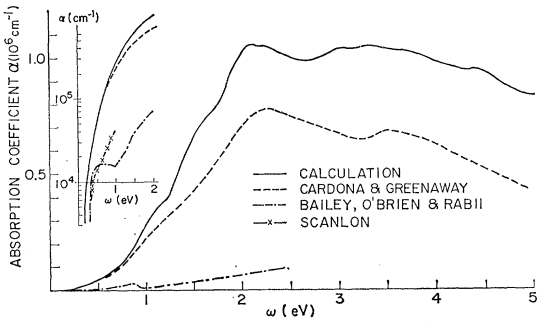

FIG. 6. The calculated absorption coefficient $\alpha(\omega)$ compared with the results of others.

obtainable due to inaccuracies in measurement of sample thickness. The scale of this curve has been adjusted to put the results in best agreement with the predictions of the KK analysis of the reflectivity.[9] The present calculation does not give the correct $\alpha(\omega)$ in the vicinity of the fundamental edge, where the absorption is very small on the scale of this figure. This is so for two reasons: (1) $\alpha(\omega)$ near the edge depends upon the details of the bands near L and requires a detailed calculation like that of Ref. 7. (2) The spectral width $h/\tau \simeq 0.07$ eV which has been given to every transition in the calculation is responsible for the fact that $\alpha(\omega)$ does not fall off quickly below the absorption edge. However, in the frequency range where absorption is large and many transitions all over the zone contribute, the present calculation is expected to be nearly correct (subject, of course, to the frequency restrictions discussed in Sec. III).

Two important observations can be made by comparing the calculations of Figs. 3–6 with the bands of Fig. 1. The first is that peaks in $\epsilon_2(\omega)$ are not associated directly with critical points in the joint density of states.[21] Although the oscillator strength for interband transitions tends to be largest near critical points, the joint density of states reaches a maximum somewhat above the critical-point energy. The second is that peaks in the reflectivity are not directly associated with peaks in $\epsilon_2(\omega)$ as pointed out by Cohen with regard to CdTe.[22] We conclude that interpretation of the reflectivity peaks in terms of associated critical points is not adequate for PbTe, and that a more comprehensive interpretation is required.

[21] For a discussion of critical-point analysis see Ref. 13, p. 67.

[22] M. L. Cohen, *II–VI Semiconducting Compounds, 1967 International Conference* (W. A. Benjamin, Inc., New York, 1967), p. 475.

In carrying out the integration on **k** space, the contribution from each region of the BZ was calculated separately (Sec. III) making it possible to identify unambiguously each contribution to the optical constants with a point in the BZ. The most important result which this analysis yields is that the optical constants receive important contributions from a large region of **k** space and not only from the region around L. This greatly complicates interpretation of the spectrum, but it explains the enormous discrepancy between the present calculation and that of Ref. 7 at frequencies above the fundamental edge. The region which makes important contributions to ϵ_2 can be visualized as a surface of minimum gap over which the gap varies but never becomes much larger than the gap at L.[23] This surface is formed by six approximately planar surfaces which are perpendicular to the six Δ axes and which intersect these axes at $\mathbf{k} \simeq \pi/a$ (0.75, 0.0, 0.0). The departure of these surfaces from planes is seen from the fact that they intersect the Σ axis at $_k \simeq \pi/a$ (0.85, 0.85, 0.0) and the Λ axis at L. Thus we see that the small gap at L is not the only reason for the strong absorption or the high optical dielectric constant ($\epsilon_\infty = 31.8$)[24] of PbTe. Because there is a large region of **k** space over which the gap is small, many transitions participate in the absorption process.

A summary of how different regions of **k** space contribute to the calculation of ϵ_2 is given in Table IV. As discussed in Sec. III, the region of integration (1/48th of the BZ) was subdivided into cubic boxes $0.4\pi/a$ on a side. Some of the boxes lie partially outside the region of integration, and their effective volume is reduced accordingly. Each box is labeled by the coordinate of its lower left-hand corner, and several of these boxes are listed in Table IV together with their effective volume and the contribution which they make to ϵ_2 at selected frequencies. Thus, even though the present

[23] The Δ- and Σ-axis gaps are found to be approximately 1.8 and 1.2 eV by P. J. Lin and L. Kleinman, Phys. Rev. **142**, 478 (1965), 2.5 and 1.3 eV by Tung and Cohen (Ref. 4), and 2.2 and 1.2 eV by Herman *et al.* (Ref. 1). This compares with 1.8 and 0.75 eV in the present work.

[24] A. K. Walton and T. S. Moss, Proc. Phys. Soc. (London) **81**, 509 (1963).

TABLE IV. Contributions to $\epsilon_2(\omega)$ from different regions of the BZ. The **k** space is subdivided into cubes $0.4\pi/a$ on a side and the subdivision labeled by the coordinates in the first column is that portion of the cube which lies within the region of integration (1/48 of the BZ). There are 24 subdivisions in all. Subdivisions not listed explicitly contribute less than unity to ϵ_2 at all frequencies. The volume of the region of integration is $1000/96 = 10\,5/12$ in these units.

Coordinate of lower left-hand corner in units of π/a	Volume in units of $(0.4\,\pi/a)^3$	Contribution to $\epsilon_2(\omega)$ at selected photon energies							
		0.4 eV	1.0 eV	1.1 eV	1.4 eV	1.8 eV	2.0 eV	3.0 eV	4.0 eV
0.4 0.0 0.0	$\frac{1}{2}$	0.015	0.064	0.082	0.213	3.423	6.673	0.186	0.245
0.8 0.0 0.0	$\frac{1}{2}$	0.004	0.013	0.017	0.035	0.316	0.937	0.465	0.190
0.4 0.4 0.0	$\frac{1}{2}$	0.093	2.779	3.073	4.496	4.399	2.845	0.870	0.371
0.8 0.4 0.0	1	0.100	2.978	3.637	3.428	3.727	4.142	0.855	0.685
0.8 0.8 0.0	$\frac{1}{2}$	0.236	8.657	12.217	6.881	4.393	3.610	1.474	0.214
1.2 0.8 0.0	$\frac{15}{16}$	0.120	0.974	1.833	14.410	8.558	4.229	0.560	0.350
1.6 0.8 0.0	$\frac{1}{2}$	0.011	0.052	0.070	0.281	2.055	1.924	0.408	0.028
0.4 0.4 0.4	$\frac{1}{6}$	0.047	1.748	2.080	1.934	1.122	0.973	0.376	0.137
0.8 0.4 0.4	$\frac{1}{2}$	0.084	3.152	3.585	2.861	2.146	2.539	1.039	0.383
0.8 0.8 0.4	$\frac{15}{32}$	1.809	12.572	9.105	4.142	6.171	3.876	1.091	0.250
1.2 0.8 0.4	$\frac{1}{2}$	0.062	1.109	2.232	5.545	2.644	2.008	0.563	0.293
0.8 0.8 0.8	$\frac{1}{12}$	6.587	1.033	0.811	1.925	0.856	0.571	0.289	0.051
Remaining regions	4 25/96	0.088	1.142	0.673	0.937	1.201	1.531	0.833	0.523
Total	10 5/12	9.256	36.273	39.415	47.088	41.011	35.858	10.009	3.720

calculation does not reliably reproduce all the peaks in the measured reflectivity,[9] this analysis enables one to determine which transitions are responsible for the optical properties at each frequency.

The E_0 shoulder in the calculated reflectivity is unambiguously identified with the fundamental edge at L. The onset of this shoulder occurs at approximately the gap frequency, and, since ϵ_2 and k are small in this range, the E_0 reflectivity shoulder occurs at nearly the same frequency (0.4 eV) as the corresponding peaks in ϵ_1 and n. At higher frequencies the interpretation of the spectrum is not so simple for reasons discussed above. However, the results of the present analysis confirm most of the interpretation given in Ref. 1.

The E_1 peak which occurs in the measured reflectivity at 1.25 eV has been assigned to the lowest $\Sigma_5 \rightarrow \Sigma_5$ transition.[1,9] In addition, electroreflectance indicates quite clearly an M_1 critical point at 1.2 eV, which is believed to correspond to this transition.[25] In the present calculation, the Σ-axis minimum is a M_1 critical point, but the gap has energy 0.75 eV and gives rise to a peak in ϵ_2 at 1.1 eV which in turn causes a peak in the calculated reflectivity at 1.1 eV. Actually this gap is indirect.[7] The conduction-band minimum occurs at a slightly different point in **k** space than the valence-band maximum as is true for all gaps which occur off high-symmetry points. However, this does not affect significantly the joint density of states for *direct* transitions which is extremely large and has a critical point which occurs at a point in **k** space between the conduction-band minimum and the valence-band maximum. As seen from Table IV the contribution to ϵ_2 at 1.1 eV is largest from the boxes having coordinates (0.8,0.8,0.0) and (0.8,0.8,0.4). The former includes the Σ-axis minimum and contributes 31% of ϵ_2; the latter is adjacent to the Σ-axis minimum and contributes 23% of ϵ_2. The relative unimportance of the region around L can be seen from the fact that the box which has coordinates (0.8,0.8,0.8) contains L and contributes only 2% of ϵ_2 at this frequency. Since the Σ-axis minimum is an M_1 critical point, the gap must be smaller off the Σ axis. In the present calculation, the gap decreases rather uniformly from the Σ-axis minimum to the L point. Thus, the point of **k** space which contributes most strongly to ϵ_2 moves with increasing frequency along the surface of minimum gap in the direction of increasing gap from L toward the Σ-axis minimum. For frequencies above 1.1 eV, several points on the surface of minimum gap contribute strongly as shown by Table IV. The peak in ϵ_2 which occurs at 1.4 eV results primarily (31%) from the box having coordinates (1.2,0.8,0.0) which is adjacent to the box containing the Σ-axis minimum. The 1.4-eV peak in ϵ_2 causes a peak in k at 1.65 eV and an associated peak in the calculated reflectivity at 1.65 eV. Thus, two peaks occur in the calculated reflectivity in this region whereas only one is observed. This discrepancy is probably due to the Σ-axis gap being too small. If this gap were slightly larger, the 1.1-eV peak would overlap the 1.4-eV peak giving a single peak at approximately the correct frequency, but the general features discussed above would remain substantially unchanged.

The E_2 peak in the reflectivity is measured at 2.4 eV and occurs at 2.55 eV in this calculation. At this frequency both n and k are varying almost linearly with frequency, but the structure can be thought of as being due to the peak in k which occurs at 2.05 eV. This peak results from the 2.10-eV minimum in ϵ_1, which is related through the KK relations to the steep decline in ϵ_2 from the 1.80-eV shoulder. This analysis is

[25] D. E. Aspnes and M. Cardona, Phys. Rev. **173**, 714 (1968).

commensurate with the electroreflectance measurements which find no critical points near the E_2 peak.[25] Detailed analysis of the 1.8-eV peak in ϵ_2 reveals that it is due to transitions from the second valence band to the primary conduction band and transitions from the primary valence band to the second conduction band in a region of $\mathbf{k}$ space which is included in the box having coordinate (0.8,0.8,0.4). The onset of these transitions occurs at L where their respective energies are 1.20 eV (L_4^+, $L_5^+ \rightarrow L_6^-$) and 1.23 eV ($L_6^+ \rightarrow L_6^-$) but, because of the joint density-of-states term, the contribution to ϵ_2 from these transitions reaches its maximum at 1.8 eV in the above-mentioned region of $\mathbf{k}$ space, which is adjacent to L. This is the only place where transitions of this type are important in the frequency range under consideration, because elsewhere in $\mathbf{k}$ space these bands are too far apart. Table IV shows that the major contribution to ϵ_2 at 2.0 eV comes from the box having coordinate (0.4,0.0,0.0) which includes the Δ-axis minimum, and above 2.0 eV ϵ_2 falls sharply.

V. CONCLUSION

The $\mathbf{k}\cdot\mathbf{p}$ secular equation in which the band parameters were calculated from APW wave functions at Γ is found to give a remarkably faithful representation of the APW energy bands elsewhere in the zone. We have used the $\mathbf{k}\cdot\mathbf{p}$ scheme to calculate the optical constants of PbTe because, using this scheme, interband momentum matrix elements are obtained directly without making any approximations other than the truncation of the secular equation.

The present calculation of $\epsilon_2(\omega)$ differs from the results of Ref. 9 by approximately a factor of 2. This discrepancy could be due to a calculated gap which is too small throughout the region of minimum gap, or it could be due to approximations in the KK analysis used to obtain ϵ_2 from the measured reflectivity. An experiment like that of Ref. 20 could resolve this question.

The calculation illustrates clearly the dangers in interpreting reflectivity peaks in terms of joint density-of-states critical points. In PbTe, where many critical points occur close together in a small energy range, the difference in energy between joint density-of-states maxima and joint density-of-states critical points together with the uncertainty in the relationship between reflectivity peaks and peaks in $\epsilon_2(\omega)$ make this kind of interpretation hazardous indeed.

The method used here for calculating $\epsilon(\omega)$ can be extended to calculate the interband electronic contribution to $\epsilon(\omega,\mathbf{q})$, that is, the electronic response to a disturbance of nonzero wave vector.[26] Using the $\mathbf{k}\cdot\mathbf{p}$ scheme, it is possible to obtain matrix elements of the operator $e^{-i\mathbf{q}\cdot\mathbf{r}}$, and the dielectric response function can be calculated for wave vectors different from zero as accurately as for $\mathbf{q}=0$. The only information which is required in addition to the $\mathbf{k}\cdot\mathbf{p}$ bands discussed above is matrix elements of $e^{i\mathbf{Q}\cdot\mathbf{r}}$ between Bloch functions at Γ, where $\mathbf{Q}$ is the reciprocal-lattice vector required to make $\mathbf{k}+\mathbf{q}+\mathbf{Q}$ fall inside the first BZ. These matrix elements can be calculated with reasonable accuracy from APW wave functions.

ACKNOWLEDGMENTS

The authors are grateful to Professor Mildred Dresselhaus and Professor George Pratt, Jr., of MIT and to Dr. Gene Dresselhaus of Lincoln Laboratory for their contribution to this work. We are also grateful to Professor Marvin Cohen and Yvonne Tsang for sending us their results on the optical constants of PbTe. This work was begun at Lincoln Laboratory.

[26] D. R. Penn, Phys. Rev. **128**, 2093 (1962); H. Nara, J. Phys. Soc. Japan **20**, 778 (1965); **20**, 1097 (1965); G. Strinivasan, Phys. Rev. **178**, 1244 (1969).